DOI: 10.1002/smll.200600147

Attachment of Streptavidin to β-Cyclodextrin Molecular Printboards via Orthogonal Host–Guest and Protein–Ligand Interactions

*Manon J. W. Ludden, Mária Péter, David N. Reinhoudt, and Jurriaan Huskens**

Streptavidin (SAv) is attached to β-cyclodextrin (β-CD) self-assembled monolayers (SAMs) via orthogonal host–guest and SAv–biotin interactions. The orthogonal linkers consist of a biotin functionality for binding to SAv and adamantyl functionalities for host–guest interactions at β-CD SAMs. SAv complexed to excess monovalent linker in solution and then attached to a β-CD SAM could be removed by rinsing with a 10 mM β-CD solution. When SAv was attached to the β-CD SAM via the divalent linker, it was impossible to remove SAv from the surface by the same rinsing procedure. This is interpreted by assuming that two SAv binding pockets are oriented towards the β-CD SAM resulting in (labile) divalent and (stable) tetravalent β-CD-adamantyl interactions for the mono- and divalent linkers, respectively. This was confirmed by experiments at varying β-CD concentrations. When the [linker]/[SAv] ratio is reduced, a clear trend in the divalent-linker case is seen: the less linker the more protein could be removed from the surface. It is proven that the orthogonality of the binding motifs and the stability of the divalent linker at the β-CD SAM allows the stepwise assembly of the complex at the β-CD SAM by first adsorbing the linker, followed by SAv. This stepwise assembly allows the controlled heterofunctionalization of surface-immobilized SAv.

Keywords:
- cyclodextrins
- host–guest systems
- proteins
- self-assembled monolayers
- surface plasmon resonance

1. Introduction

The attachment of proteins at surfaces is important for various fields, such as bioanalytical, biochemical, and biophysical research.[1–6] A strong attachment between the protein and the surface is deemed essential, as well as that binding at the surface being specific, and the biomolecule of interest not being denatured at the surface.[6] Furthermore, proteins are often used as building blocks at surfaces for the build-up of larger structures.[7,8] The precise and controlled attachment of biomolecules is also a key issue in biotechnology. Streptavidin (SAv) often serves as a model protein in such studies, because of its robustness and its extensive characterization.[9–18]

There are several methods by which proteins can be attached to a surface, such as covalent attachment through

[*] M. J. W. Ludden, Dr. M. Péter, Prof. Dr. D. N. Reinhoudt, Prof. Dr. J. Huskens
Laboratory of Supramolecular Chemistry and Technology
MESA+Institute for Nanotechnology
University of Twente, P.O. Box 217
7500 AE Enschede (The Netherlands)
Fax: (+31) 53–489–4645
E-mail: j.huskens@utwente.nl
Prof. Dr. J. Huskens
MESA+Strategic Research Orientation "Nanofabrication"
MESA+Institute for Nanotechnology
University of Twente, Enschede (The Netherlands)

Supporting information for this article is available on the WWW under http://www.small-journal.com or from the author.

small NANO MICRO

primary amines at the protein surface,[19] attachment via a biochemically engineered His_6-tag at the protein to a nickel(II)-complexed nitrilo triacetate (NiNTA) linker,[20–24] or via a SAv–biotin linkage.[7] In most of these methods, however, the kinetics and thermodynamics of adsorption and desorption cannot be controlled at will. In the NiNTA–His-tag system,[24,25] however, multivalent chelator head groups can be applied, and thus proteins can be immobilized at NiNTA surfaces with high affinities, specificities, and well-defined stoichiometries.

Monolayers of biotin have previously been employed for the attachment of SAv to surfaces.[7,26–31] In these studies, it has been shown that the attachment of SAv to a biotin monolayer occurs through the use of two biotin binding pockets of SAv, and that the two remaining biotin binding pockets are available for further functionalization with biotinylated (bio)molecules. Such SAv monolayers therefore can serve as platforms for further biofunctionalization, for example, for the development of hormone sensors, as shown by Knoll et al.[7]

β-Cyclodextrin (β-CD) is a well known host for various small hydrophobic organic molecules in aqueous environments.[32] β-CD has been modified by us with seven heptathioether chains[33] in order to obtain self-assembled monolayers (SAMs) on gold. Such SAMs are ordered and densely packed, and have been extensively characterized.[33,34] Binding constants of monovalent guest molecules to a single β-CD cavity of these SAMs are comparable to binding constants of the respective molecules to β-CD in solution.[1,34] All guest-binding sites in the β-CD SAM are equivalent and independent. The use of multivalent[35] host–guest interactions allows the formation of kinetically stable assemblies, and thus local complex formation for example, by patterning, so that these surfaces can be viewed as "molecular printboards".[36,37] By choosing the correct number and type of guest sites, it is possible to control thermodynamics, kinetics, and stoichiometry of the adsorption and desorption of multivalent molecules at such surfaces.

The aim of this work is the controlled attachment of a protein to a surface with respect to kinetics, thermodynamics, and orientation, and with the potential for stimulated desorption.[38] Through the stepwise assembly of SAv to the β-CD SAM, controlled heterofunctionalization of SAv is possible (which is impossible in solution), with the potential to control the orientation of the protein towards the surface upon immobilization. Firm attachment of the protein to the surface is achieved by using appropriately functionalized linkers, while the protein is still in a liquidlike environment. In this paper, the attachment of SAv to β-CD SAMs through host–guest interactions using orthogonal linkers is discussed. The aim is to combine the robust, well-known SAv–biotin interaction motif for the formation of protein constructions with the versatility of the β-CD host–guest interaction motif for tuning the kinetics, thermodynamics, and orientation of the immobilized SAv to the β-CD SAM. Therefore, two linkers were developed, both with a biotin functionality to enable binding to SAv, and with one or two adamantyl functionalities to enable binding to the β-CD SAM. Surface plasmon resonance (SPR) spectroscopy, atomic force microscopy (AFM), X-ray photoelectron spectroscopy (XPS), and fluorescence spectroscopy were employed 1) to probe specificity of the interactions, 2) to investigate the orthogonality of the binding motifs, 3) to study the adsorption and desorption properties of the SAv–linker complexes, 4) to probe the different assembly schemes for SAv attachment, and 5) to show the possibility of controlled heterofunctionalization of SAv when immobilized to the surface in a stepwise manner.

2. Results and Discussion

For the attachment of SAv (Figure 1, **6**) at β-CD SAMs, two orthogonal linkers were developed, each with a biotin functionality to enable binding to SAv, and one (**3**) or two (**4**) adamantyl functionalities to enable host–guest interactions at the β-CD SAM. The syntheses of **3** and **4** are outlined in Scheme 1. The syntheses of **7** and **10** were performed according to literature procedures.[39] The monovalent linker (**3**) was synthesized from **7** in three subsequent steps. The bromide functionality of the monoadamantyl-functionalized tetra(ethylene glycol) bromide (**7**) was converted into a phthalimide functionality upon reaction with

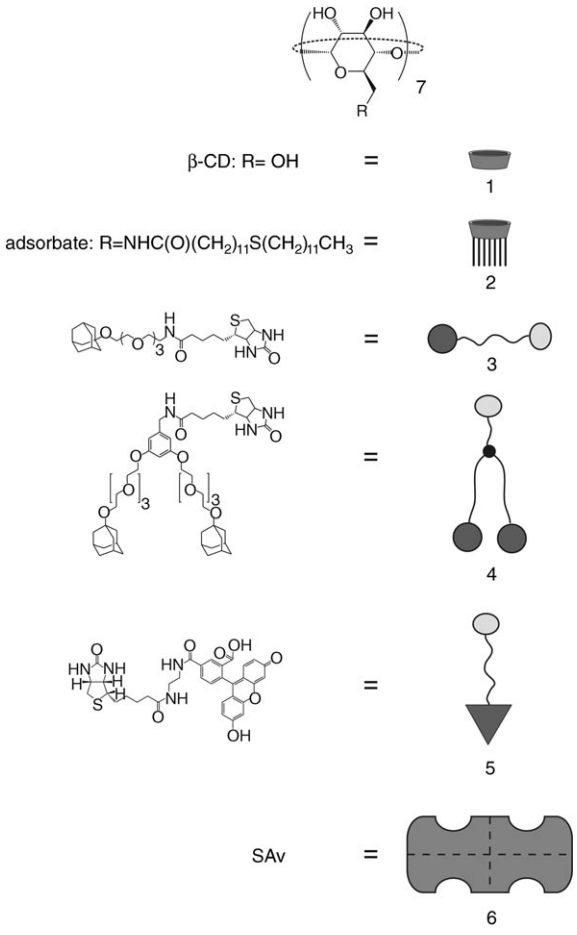

Figure 1. Building blocks used in this study: β-CD (**1**), adsorbate for preparing β-CD SAMs (**2**), monovalent linker (**3**), divalent linker (**4**), biotin-4-fluorescein (**5**), and SAv (**6**).

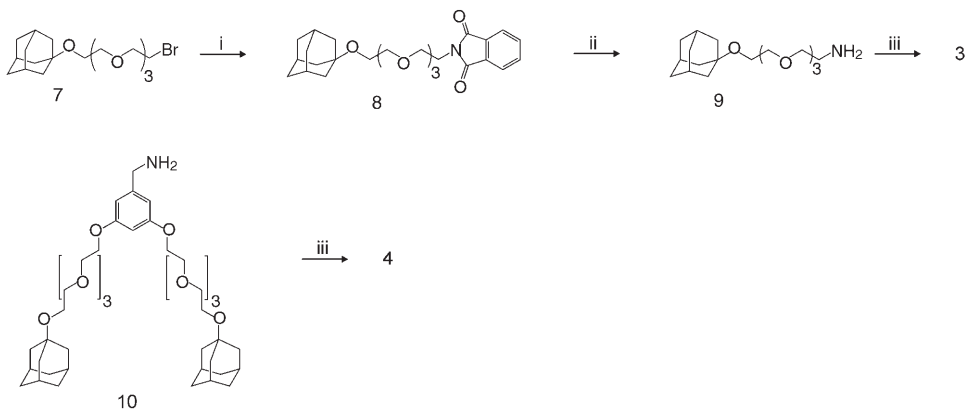

Scheme 1. Synthesis routes towards the monovalent and divalent linkers **3** and **4**: i) potassium phthalimide in dimethylformamide (DMF), 60 °C, stirring overnight; ii) $N_2H_4{\cdot}H_2O$ in ethanol, reflux, stirring overnight; iii) (+)-biotin-4-nitrophenyl ester in DMF and Et_3N, room temperature, stirring overnight.

potassium phthalimide in toluene to yield **8**. The phthalimide functionality was converted into an amino group upon reaction with hydrazine monohydrate in ethanol to yield **9**. Upon reaction of **9** with (+)-biotin 4-nitrophenyl ester, the linker **3** was obtained. The divalent linker (**4**) was prepared from **10** in one step, upon reaction with (+)-biotin 4-nitrophenyl ester.

Scheme 2 shows the various adsorption modes that can be envisaged for the adsorption of SAv to the β-CD SAM. The potential advantage of using orthogonal interactions is that the order of putting together the interaction motifs can be varied. The consequence of this versatility for our system is that the linkers can be bound in solution to SAv by the biotin–SAv interaction followed by adsorption to the β-CD SAM (Scheme 2, routes A and B), or that the linkers can be first adsorbed to the β-CD SAM followed by SAv attachment (Scheme 2, routes C and D). For studying assembly schemes A and B, β-CD SAMs on gold were placed in a flow cell and studied by surface plasmon resonance (SPR) spectroscopy. Protein and linker were dissolved together in 10 mM phosphate buffered saline (PBS). The protein concentration used was 1.3×10^{-7} M, while the linker concentration was 1×10^{-4} M, unless stated otherwise. This large linker-to-protein ratio ensures that all biotin binding pockets of SAv are occupied. All solutions were passed over the β-CD SAM through the liquid cell, and the flow rate was controlled by a peristaltic pump.

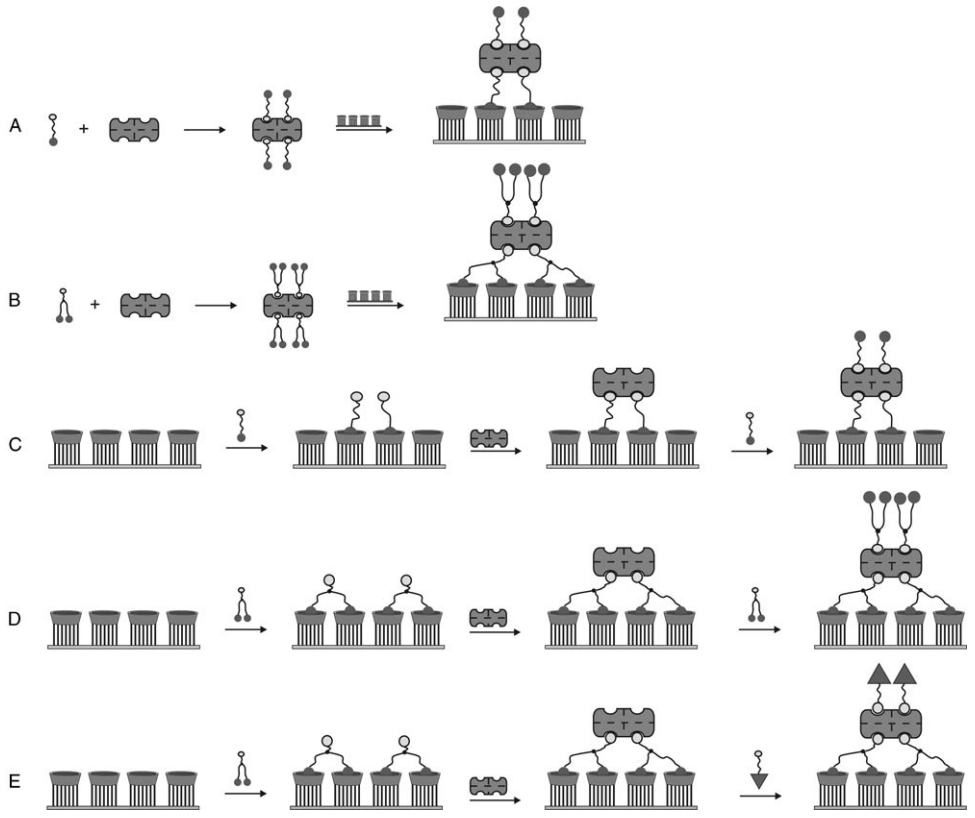

Scheme 2. Adsorption schemes for the assembly of SAv at β-CD SAMs through monovalent and divalent linkers.

For the specific attachment of SAv to β-CD SAMs via orthogonal linkers, the reduction of nonspecific adsorption is very important. Therefore, several SPR experiments were performed to investigate the conditions for reducing or eliminating nonspecific interactions of SAv to the surface. Nonspecific adsorption of SAv to the β-CD SAM is dependent on the flow rate (data not shown). When flow rates below 0.4 mL min^{-1} were used, the nonspecific adsorption of SAv appeared to be considerable. Flow rates of 0.4 mL min^{-1} or higher reduced the nonspecific adsorption to the surface to some extent. Therefore, all subsequent experiments were performed at a flow rate of 0.5 mL min^{-1}. Nonspecific adsorption of SAv still occurred, and rinsing with a 10 mM β-CD

NANO MICRO small

solution led only to partial restoration of the signal (Figure 2, black curve). An experiment in which SAv was saturated with 1×10^{-4} M natural biotin (Figure 2, dark gray curve) showed much less nonspecific adsorption. Similarly, adsorption of SAv at a 1 mM β-CD background (light gray curve) showed that the nonspecific interactions of SAv to the β-CD SAM were strongly reduced, most likely through competition introduced by β-CD in solution.

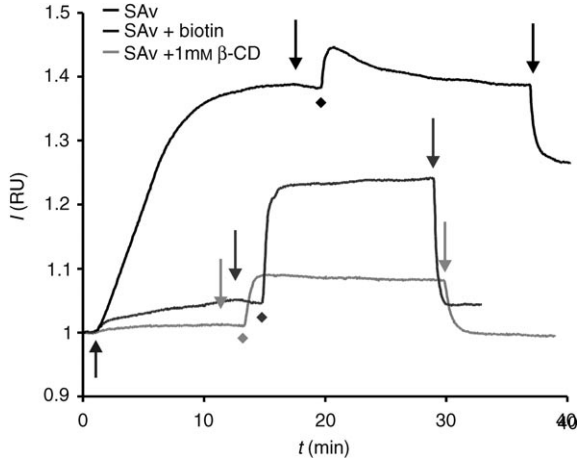

Figure 2. SPR sensograms recorded for the adsorption and (attempted) desorption of SAv in the absence (black curve, uppermost) or presence of 1×10^{-4} mM biotin (dark gray curve, middle) or 1 mM of β-CD (light gray curve). Symbols indicate switching of solutions in the SPR flow cell: SAv with or without biotin or β-CD in PBS (↑), PBS (↓), 10 mM β-CD in PBS (◆).

In order to test the binding specificity of the linkers towards the β-CD SAM, the adsorption of each linker to β-CD SAMs was compared to their adsorption to 11-mercapto-1-undecanol SAMs. Such OH-terminated SAMs resemble the β-CD SAMs regarding polarity, but lack the specific host–guest recognition sites. Figure 3 shows the SPR sensograms of these adsorption experiments. From Figure 3 it is clear that none of the linkers adsorbed to the OH-terminated SAMs. Both linkers however did adsorb to the β-CD SAMs. This implies that the β-CD cavity is needed to ensure binding of the linkers, and thus that the adsorption of the linkers to the β-CD SAMs is specific.

Figure 4 (top) shows six SPR sensograms representing the adsorption of the SAv, bound to the monovalent linker (**3**) in solution (at β-CD concentrations ranging from 0 to 10 mM) to the β-CD SAM. It can be seen that when the β-CD concentration in the buffer was increased, less SAv adsorbed to the surface. When the SAv–monovalent linker complex was passed over the β-CD surface at low β-CD concentrations, followed by a rinsing procedure with 10 mM β-CD, the baseline was restored. In contrast, when the SAv–monovalent linker complex was passed over the surface at higher β-CD concentrations, some SAv remained at the surface.

Figure 4 (bottom) shows the SPR sensograms for the adsorption of SAv (coupled to the divalent linker (**4**) in solu-

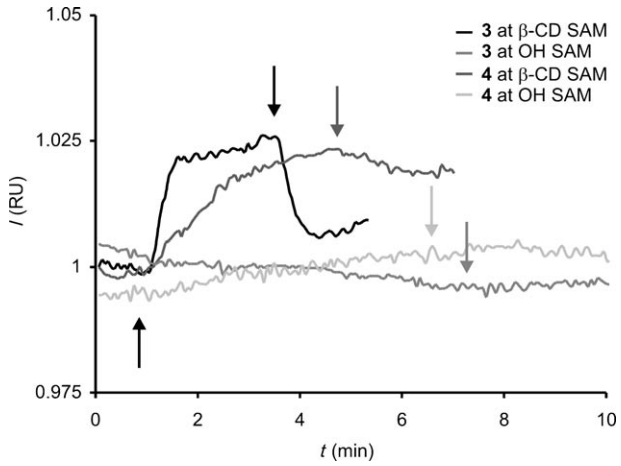

Figure 3. SPR sensograms recorded for the adsorption and (attempted) desorption of the monovalent and divalent linkers to β-CD and 11-mercapto-1-undecanol SAMs in PBS buffer with 1 mM β-CD. Symbols indicate switching of solutions in the SPR flow cell: linker with or without 1 mM β-CD in PBS (↑), PBS or 1 mM β-CD PBS (↓).

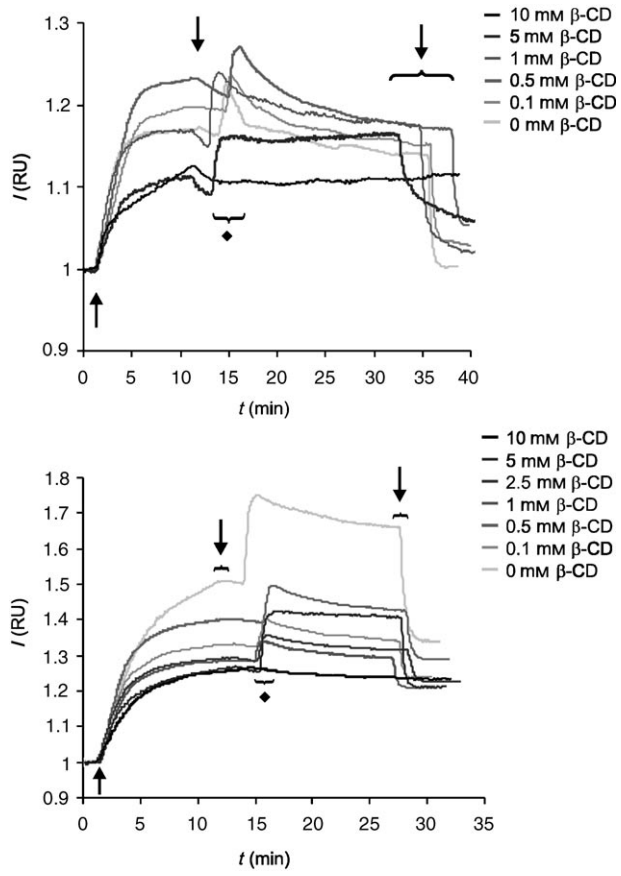

Figure 4. SPR sensograms recorded for the adsorption and (attempted) desorption of SAv complexed to monovalent linker **3** (top) and divalent linker **4** (bottom) at β-CD SAMs at increasing β-CD concentrations. Symbols indicate switching of solutions in the SPR flow cell: SAv with mono- or divalent linker in PBS (↑), PBS (↓), or 10 mM β-CD in PBS (◆).

tion) on the β-CD printboard at β-CD concentrations from 0 to 10 mM. At all β-CD concentrations the SAv–divalent linker complex adsorbed to the surface in comparable amounts. After a rinsing procedure with 10 mM β-CD in solution, it appeared impossible to remove the protein–divalent linker complex from the surface.

From Figure 4, it can be concluded that SAv can be attached to the β-CD SAM at all β-CD concentrations with either the mono- or divalent linker. This emphasizes the importance of the presence of host–guest interactions between the adamantyl functionalities of the linker and the β-CD cavity at the SAM. When SAv was attached through the monovalent linker to the β-CD SAM at lower β-CD concentrations, all attached material could be removed from the surface; at higher β-CD concentrations, most material remained. When the divalent linker was used for attachment, the complex could not be removed from the surface through competition with 10 mM β-CD. This difference in binding behavior between mono- and divalent linkers can be explained by examining the valency of the SAv/linker complexes at the β-CD SAM. When SAv is complexed with the monovalent linker in solution, four adamantyl functionalities are present at the complex (Scheme 2A). From previous studies, it is known that a compound attached to the β-CD SAM via four or more adamantyl functionalities cannot be removed from the surface through competition with a high concentration of β-CD in solution.[40] Thus, if the adsorbed protein can be desorbed, it must be bound through one to three interactions. The most likely number of interactions, however, will be two, since that corresponds with the expected orientation of SAv with two of its four binding pockets towards the surface (Scheme 2A). Complexation of the divalent linker to SAv results in a complex with eight adamantyl functionalities. Analogously this complexation is expected to be tetravalent at the β-CD SAM interface (Scheme 2B), which is in agreement with the observation that it cannot be removed from the surface. Thus, this method allows switching between reversible and irreversible complexation to the surface, simply by changing the valency of the host–guest interactions directed towards the surface.

To further investigate the valency effect of the linker on the adsorption of SAv to the β-CD SAM, two SPR titrations were performed in which the concentration of SAv was kept constant at 1.3×10^{-7} M and the concentration of the linker was increased stepwise from 0.77 to 7.7 equivalents for the monovalent linker and from 0.38 to 7.7 equivalents for the divalent linker. For both the monovalent and divalent linkers, the experiments were performed at a β-CD concentration of 1 mM to suppress nonspecific adsorption of SAv to the surface. The SPR sensograms at varying monovalent linker-to-SAv ratios are shown in Figure 5 (top). SAv was complexed to linker **3** in solution. Figure 5 (top) shows that after adsorption, it is only at the highest linker concentration that the original baseline was restored after desorption by inducing competition with 10 mM β-CD. At lower linker concentrations the complex also adsorbed at the surface, but after inducing competition with 10 mM β-CD, some of the complex remained. The SPR sensograms at varying divalent linker-to-SAv ratios are shown in Figure 5 (bottom).

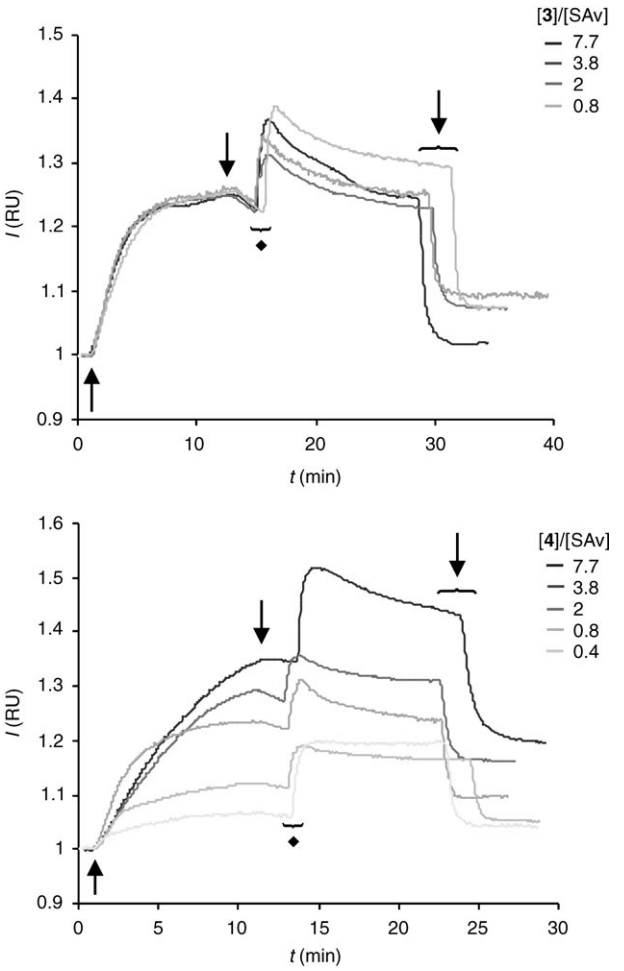

Figure 5. SPR sensograms recorded for the adsorption and (attempted) desorption of SAv at an increasing [**3**]/[SAv] ratio (top) and [**4**]/[SAv] ratio (bottom). Symbols indicate switching of solutions in the SPR flow cell: SAv–linker in 1 mM β-CD PBS (↑), 1 mM β-CD PBS (↓), 10 mM β-CD in PBS (◆).

SAv was complexed to the divalent linker **4** in solution as well. In this case, adsorption was stronger at higher linker concentrations and, under all conditions, only relatively small fractions could be removed.

The SPR sensograms confirmed that there is a difference in binding of SAv to the β-CD SAM between the mono- and divalent linkers in these concentration series. When SAv is adsorbed to the surface using the monovalent linker, the binding of the SAv–monovalent linker complex to the surface is reversible at high linker concentrations, because it can be removed after adsorption by competition with 10 mM β-CD in solution. At lower concentrations of the monovalent linker, however, more nonspecific interactions are apparent, leading to only partial removal of the monovalent linker–SAv complex from the surface. This is most likely caused by the presence of empty SAv binding pockets at low linker concentrations. When SAv is adsorbed to the surface through the divalent linker, the adsorption at higher linker concentrations is stronger, due to the formation of specific tetravalent interactions. The complex cannot

NANO MICRO small

be removed, neither at high concentrations because of the high valency, nor at low concentrations due to nonspecific interactions.

As a last test, the SAv–linker complexes were built up at the surface in a stepwise fashion (Scheme 2, routes C and D). In these experiments, a β-CD concentration of 1 mM in PBS was used to suppress nonspecific adsorption of SAv to the surface. First, the linker was allowed to flow over the surface, followed by SAv, and finally the linker again, to occupy the free biotin-binding sites at the SAv side exposed to the solution. In Figure 6, the combined SPR graphs are depicted. After adsorption of the monovalent linker **3** (gray line, Scheme 2C), the baseline was restored upon rinsing with 1 mM β-CD. When SAv was passed over this surface, only some nonspecific adsorption was observed. When the linker was passed over this surface again, it reversibly adsorbed to the surface in a fashion comparable to the initial linker adsorption, indicating that many CD sites were still accessible. For the divalent linker (black line; Scheme 2D), it can be seen that the linker remained at the surface after adsorption and rinsing with buffer containing 1 mM β-CD. When SAv was subsequently allowed to flow over the surface, a strong adsorption was observed. After adsorption of SAv, the divalent linker was passed over the SAv surface, and this adsorption was again irreversible. Thus it is clear that only the divalent linker allows a reliable stepwise build-up of the SAv complex and thus a controlled functionalization of sides of SAv, potentially with two different linkers.

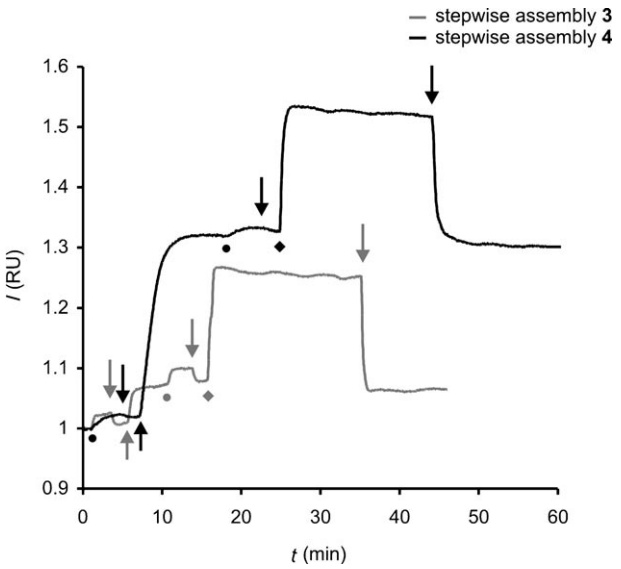

Figure 6. SPR sensograms for the stepwise adsorption of the SAv–linker complex at the β-CD SAM. The black and gray curves represent the adsorption via the mono- and divalent linkers, respectively. Symbols indicate switching of solutions in the SPR flow cell: linker (●), SAv (↑), PBS containing 1 mM β-CD (↓), PBS containing 10 mM β-CD (◆).

XPS studies were performed in order to follow the different adsorption steps. Therefore a β-CD SAM, a β-CD SAM fully covered with divalent linker, and then same system with SAv adsorbed on top were studied by XPS. Although the absolute values differed considerably from the theoretically expected values, we could conclude from the relative trends (see Supporting Information) that the organic layer thickness increased in each adsorption step, as indicated by the decrease of the Au 4f signal. Upon protein adsorption, the N 1s signal increased, confirming the adsorption of SAv.

The stepwise assembly of SAv can be extended to the patterning of β-CD SAMs. Patterned surfaces were obtained by microcontact printing (μCP) the divalent linker onto β-CD SAMs, and subsequently flowing SAv over the sample. The adsorption of SAv to the specifically patterned surface was followed in situ by an atomic force microscope equipped with a liquid cell. Imaging in a liquid cell not only allows the possibility of following the adsorption of SAv in situ in a liquidlike environment, but also ensures the monitoring of the process at the very same spot. Another advantage is that, due to imaging in a liquid, capillary forces are excluded; therefore the forces exerted by the scanning tip to the surface are at least two orders of magnitude less than in air. Potential damage to the protein layer is minimized this way.

Polydimethylsiloxane (PDMS) stamps were treated with ozone and UV irradiation to render them hydrophilic, and placed in a 1×10^{-4} M aqueous solution of the divalent linker. Subsequently, the stamps were blown dry in a stream of N_2, and placed in contact with the β-CD SAMs on gold. The samples were rinsed with water, dried, and before assembling them into the liquid cell they were imaged by contact-mode AFM in air in order to verify the presence and quality of the divalent linker patterns (Figure 7a, left). The height of the patterns from the topography image shown in Figure 7a was estimated by cross-section analysis to be about 0.5 nm (Figure 7a, right). This corresponds to the theoretically expected height of the adsorbed divalent linker.

Subsequently, the samples were assembled into a liquid cell filled with deionized water, and again height images were recorded in contact mode (Figure 7b, left). After this step, 10 mL of SAv (5×10^{-7} M) was passed through the cell with a 1 mM background concentration of β-CD in order to suppress nonspecific interactions. Afterwards, water was passed through the cell and AFM images were recorded in contact mode (Figure 7c, left). The cross-section analysis of the AFM image gave a height of about 2.7 nm (Figure 7c, right), indicating the successful adsorption of SAv. Subsequently, 10 mM β-CD was allowed to flow through the liquid cell followed by flushing with water and again an AFM height image was recorded in water. After this last rinsing step, a slight decrease in height was observed. Initially this was attributed to material removal by rinsing with β-CD, but zooming out to a larger scan area showed that the height decrease was present only in the initially scanned area where we initially scanned for a longer time (see Supporting Information). Thus, the decrease in height is attributed to some compression or removal of the protein by the scanning tip. The AFM experiments showed that the attachment of SAv only occurred at the areas prepatterned by the divalent linker. There were no signs of nonspecific SAv ad-

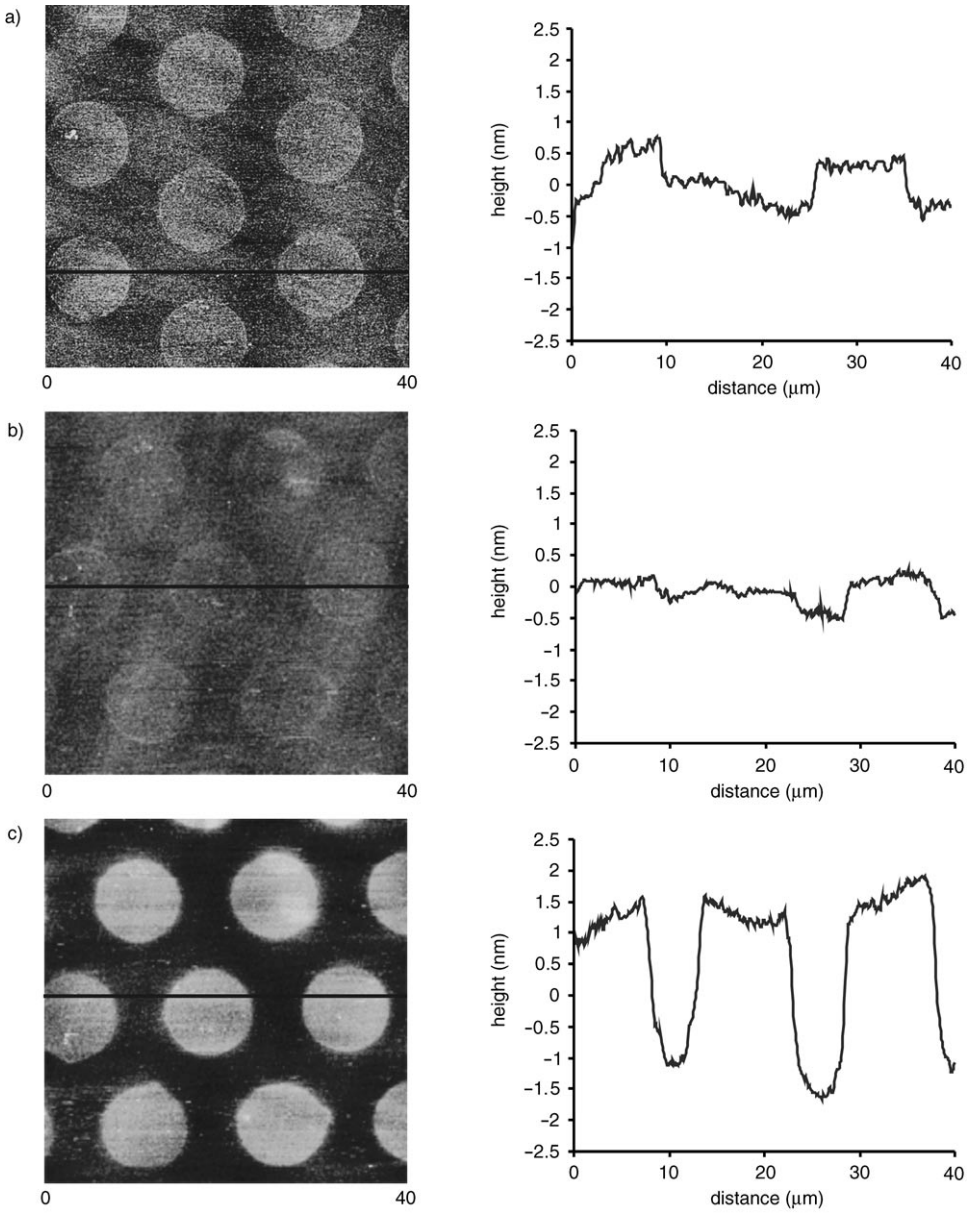

Figure 7. Contact-mode AFM height images (left; z range = 5 nm) with cross sections performed across the shown lines (right) recorded in air (a) or water (b, c) after printing the divalent linker **4** onto the β-CD SAM (a), after transfer of the sample to water (b), and after subsequent SAv adsorption (c).

face. The samples were dried in a stream of N_2, and examined by fluorescence microscopy. Figure 8a confirms the results obtained by SPR experiments in which the SAv complex was built up at the surface in a stepwise manner. The fluorescence patterns clearly indicate the presence of free binding pockets available for subsequent biotin binding after the SAv assembly step. The complete absence of fluorescence in the noncontacted areas shows the excellent specificity of the binding of the fluorescent-labeled biotin. Figure 8b shows a fluorescence image of the same process, but without SAv attachment. The absence of a pattern confirms again the specific interactions between SAv and the fluorescently labeled biotin that are needed to create the pattern.

3. Conclusions

It has been shown that it is possible to attach a protein (in this case SAv) to β-CD SAMs through orthogonal host–guest and protein–ligand interactions. Both the mono- and divalent linkers (**3** and **4**) can be used in this assembly process, as shown by SPR. It was possible to reduce nonspecific interactions between SAv and the β-CD SAM by adding 1 mM β-CD. Also, nonspecific interactions were reduced when all biotin-binding pockets of SAv were occupied. From SPR experiments in which the β-CD concentration or the [linker]/[SAv] ratio was varied, it was concluded that when the monovalent linker is used, SAv is complexed to the surface through two adamantyl–cyclodextrin interactions, while in the case of the divalent linker, the binding was tetravalent. We have also examined the assembly of the protein–divalent linker complex in a stepwise fashion at the surface, leaving the upper two binding pockets of SAv available for further (hetero)-functionalization. This scheme was not possible with the monovalent linker, because the binding of this linker to the

sorption on the bare β-CD sites, indicating excellent specificity under these conditions.

In order to show controlled heterofunctionalization at the stepwise immobilized SAv, an experiment was performed in which the divalent linker was printed onto a β-CD SAM on glass (Scheme 2E). SAv was attached on top of the linker, followed by the attachment of fluorescein-labeled biotin. Cyclodextrin SAMs on glass were prepared as described before.[41] Printing of the divalent linker **4** was performed as described above for the patterning of β-CD SAMs on gold. The patterned substrates were placed in a liquid cell, and for one sample SAv was allowed to flow over the substrate at a β-CD concentration of 1 mM. Subsequently fluorescein-labeled biotin was passed over the sur-

NANO MICRO small

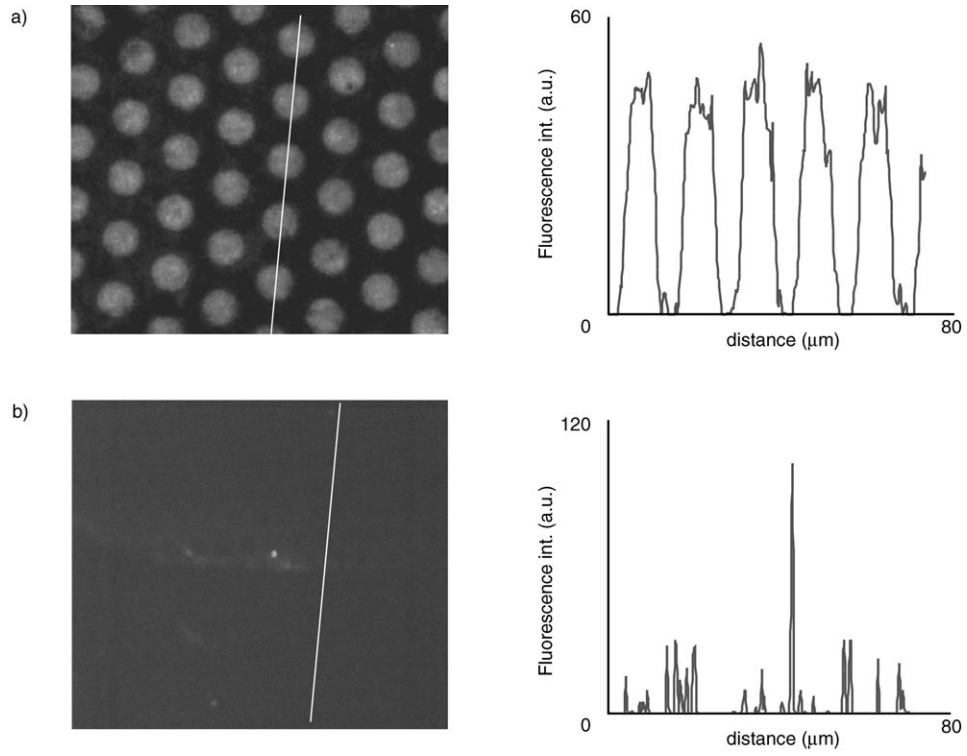

Figure 8. a) Fluorescence image and line scan recorded after printing the divalent linker **4** followed by the selective attachment of SAv to the patterned areas, and subsequent attachment of fluorescein-labeled biotin to the available biotin binding pockets at SAv; b) fluorescence image and line scan recorded after printing the divalent linker **4**, and subsequent flow of fluorescein-labeled biotin over the patterned surface.

surface is not thermodynamically strong enough. The stepwise assembly of SAv to the β-CD SAM was also proven by AFM imaging, from which it was concluded that the height of the SAv–linker complex attached to the β-CD SAM is about 2.7 nm. From experiments with fluorescently labeled biotin, it was shown that the upper biotin binding pockets were indeed available for further functionalization, in this case also providing controlled heterofunctionalization. Both AFM imaging and fluorescence studies showed that the attachment of SAv was very specific, and that there was no detectable nonspecific interaction of SAv to the β-CD SAM.

The approach used here for the attachment of SAv to a surface shows that multivalency plays an important role in the adsorption of proteins to surfaces. The stepwise adsorption of SAv to the surface through the divalent linker enables us to use the biotin binding pockets that are directed towards the solution for the binding of other, biotinylated (bio/macro)molecules. β-CD is a cyclic oligosaccharide, and interactions between the hydrophobic β-CD cavity and hydrophobic amino acids of proteins will occur.[42–44] However, this appeared not to interfere with the biomolecules used in this system. It is difficult to predict whether β-CD will interfere with other biological systems, but in the case of stepwise assembly onto the SAv layer by the further (hetero)-functionalization of the free binding pockets, β-CD does not need to be present. The approach presented here can be used for further build-up and patterning of (bio)molecular nanostructures at interfaces, especially by further functionalization of the unused biotin binding sites of SAv immobilized during the stepwise fabrication procedure.

4. Experimental Section

General: All materials and reagents were used as received, unless stated otherwise. The syntheses of **7** and **10** have been reported previously.[39] Biotin-4-fluorescein was bought from Sigma and used as received. All moisture-sensitive reactions were carried out under an argon atmosphere. ^{1}H NMR spectra were recorded on Bruker AC300 and AMX400 spectrometers. Spectra are reported in ppm downfield from trimethylsilane (TMS) as an internal standard. Mass spectrometry (MS) measurements (fast atomic bombardment, FAB-MS and matrix-assisted laser desorption ionization time-of-flight, MALDI-TOF-MS) were recorded with a Finnigan MAT 90 spectrometer using *m*-NBA as a matrix and a PerSpective Biosystems Voyager-De-RP spectrometer, respectively. Analytical thin-layer chromatography (TLC) was performed using Merck-prepared plates (silica gel 60 F-254 on aluminum). Merck silica gel (40–63 μm) was used for flash chromatography.

*Triethylene glycol phthalimide-ethyl adamantyl ether (**8**)*: Compound **7** (1.02 g, 2.6 mmol) and potassium phthalimide (482 mg, 2.6 mmol) were mixed in DMF (30 mL) and allowed to reflux for 10 h while stirring. The precipitate was filtered off after cooling to room temperature, and the solvent was removed by rotary evaporation. The product was a yellowish oil (yield 75%).

^{1}H NMR (300 MHz, $CDCl_3$, 20 °C, TMS): δ (ppm): 7.90 (m, 2H, ArH), 7.70 (m, 2H, ArH), 3.86 (t, 2H, AdO$CH_2$$CH_2$), 3.75–3.70 (t, 2H, N$CH_2$$CH_2$), 2.65–2.55 (m, 12H, O$CH_2$$CH_2$O), 2.15 (m, 3H, $CH_2$$CH$$CH_2$Ad), 1.76–1.75 (m, 6H, CHCH_2CAd), 1.64–1.58 (m, 6H, CHCH_2CHAd); ^{13}C NMR: δ (ppm): 169.0, 132.1, 127.6, 70.5, 70.2, 67.8, 66.1, 43.1, 39.2, 38.1, 36.4, 30.4; MS (FAB-MS): *m/z* calcd for $[M+H^+]$ 458.3, found 458.3.

*Triethylene glycol amine-ethyl adamantyl ether (**9**)*: Compound **8** (1.4 g, 3.05 mmol) was dissolved in ethanol. The mixture was heated to reflux and hydrazine monohydrate (0.168 g, 3.36 mmol) was added. The mixture was allowed to reflux for 1 h. Thereafter, the mixture was allowed to cool to room temperature, and 6 M hydrochloric acid was added to obtain a slightly acidic solution. Subsequently, the mixture was refluxed for 1 h.

After cooling to room temperature the phthalhydrazine was filtered off, and the remaining liquid was removed by rotary evaporation. The product was a colorless oil (yield 90%).

^{1}H NMR (300 MHz, $CDCl_3$, 20 °C, TMS): δ (ppm): 3.75–3.50 (m, 16H, OCH_2CH_2O + O$CH_2CH_2NH_2$), 2.85 (t, 2H, CH_2NH_2), 2.15 (m, 3H, CH_2CHCH_2Ad), 1.76–1.75 (m, 16H, CHCH_2CAd), 1.64–1.58 (m, 6H, CHCH_2CHAd); ^{13}C NMR: δ (ppm): 73.9, 73.7, 73.3, 69.0, 68.5, 67.5, 66.5, 66.3, 66.1, 65.9, 57.5, 55.5,37.8, 32.5, 26.8; MS (FAB-MS): *m/z* calcd for [M+H$^+$] 327.2, found 327.5.

*Triethylene glycol biotin-ethyl adamantyl ether (**3**)*: Compound **9** (297 mg, 0.65 mmol) was dissolved in DMF (2 mL) and Et_3N (0.1 mL, 0.72 mmol). Then, (+)-biotin-4-nitro-phenyl ester (238 mg, 0.65 mmol) was added to this solution, which was then stirred overnight at room temperature. Subsequently, diethyl ether was added dropwise, and the product precipitated. The product was redissolved in DMF, and precipitated again by adding diethyl ether dropwise. The product was recovered as a white solid (yield 60%).

^{1}H NMR (400 MHz, D_2O, 20 °C, TMS): δ (ppm): 6.80 (t, 2H, CO*NH*), 5.60 (s, 2H, CH_2NHCH_2), 4.45 (m, 1H, NHCHCH$_2$), 4.25 (m, 1H, NHCHCH), 3.65–3.45 (m, 12H, OCH_2CH_2O), 3.39 (m, 2H, CH_2NHCO), 3.10 (m, 1H, CHCHCH$_2$), 2.85 (d, 1H, SCH_2CH), 2.65 (s, 1H, SCH_2CH), 2.10 (t, 2H, COCH_2CH_2), 2.05 (m, 3H, CH_2CHCH_2Ad), 1.75–1.45 (m, 12H, CHCH_2CAd + $CH_2CH2CH2CH2$CH), 1.60–1.58 (m, 6H, CHCH_2CHAd); ^{13}C NMR: δ (ppm): 170.0, 73.8, 73.4, 73.3, 68.9, 67.5, 66.8, 66.3, 58.0, 56.5, 55.5, 54.5, 51.9, 49.5; MS (MALDI-TOF-MS): *m/z* calcd for [M+H$^+$] 553.8, found 553.2.

*1-Biotin-3-(3,5-di(tetraethylene glycol adamantyl ether) benzyl amide (**4**)*: Compound **10** (250 mg, 0.33 mmol) was dissolved in DMF, and a few drops of triethylamine were added, followed by (+)-biotin-4-nitro-phenyl ester (238 mg, 0.65 mmol). The mixture was stirred overnight at room temperature. The product was precipitated by adding diethyl ether dropwise. The product was redissolved in DMF and precipitated again by adding diethyl ether dropwise (three times). The product was recovered as a white solid (yield 55%).

^{1}H NMR (400 MHz, $CDCl_3$, 20 °C, TMS): δ (ppm): 6.55 (s, 2H, ArH), 6.39 (s, 1H, ArH), 4.49 (t, 2H, NCHCH + NCHCH$_2$), 4.13 (t, 4H, ArOCH_2), 3.86 (m, 6H, AdOCH_2 + CCH_2NH), 3.76–3.65 (m, 18H, OCH_2CH_2O + CCH_2NH), 3.60 (m, 8H, AdOCH$_2CH_2$ + CH_2CH_2OAr), 2.16 (m, 3H, CH_2CHCH_2Ad), 1.75–1.76 (m, 18H, CHCH_2CAd + $CH_2CH_2CH_2CH_2$CH), 1.68–1.58 (m, 12H, CHCH_2CHAd); ^{13}C NMR: δ (ppm): 162.0, 160.0, 105.0, 82.0, 80.5, 79.2, 78.0, 77.5, 71.2, 70.5, 69.5, 68.8, 67.0, 61.0, 58.8, 56.0, 55.5 ppm; MS (MALDI-TOF-MS): *m/z* calcd for [M+H$^+$] 987.3, found 987.2.

Monolayer preparation: Gold substrates for SPR (BK7 glass/2–4 nm Ti/50 nm Au), XPS (BK7 glass/2–4 nm Ti/200 nm Au) and AFM (Si wafer/2–4 nm Ti/20 nm Au) were obtained from SSens B.V., Hengelo, The Netherlands. Gold substrates were cleaned by dipping them in piranha solution (1:3 mixture of concentrated H_2SO_4 and 30% H_2O_2) for 5 s (*WARNING:* piranha solution should be handled with caution; it can detonate unexpectedly). After thorough rinsing with Millipore water, they were placed for 10 min in absolute ethanol in order to remove the oxide layer. Subsequently the substrates were placed in a freshly prepared solution of β-CD heptathioether (**2**; 0.1 mM) for 16 h at 60 °C. The samples were subsequently rinsed three times with $CHCl_3$, ethanol, and Millipore water.[33] The 11-mercapto-1-undecanol SAMs were prepared by leaving clean gold substrates in an ethanolic solution of 11-mercapto-1-undecanol overnight. The layers were rinsed three times with dichloromethane, ethanol, and Millipore water. All solvents used in the monolayer preparation were of analytic grade. β-CD monolayers on glass were prepared as described previously.[41]

SPR spectroscopy: SPR measurements were performed on a Resonant Probes Gmbh SPR instrument. The instrument consists of a HeNe laser (JDS Uniphase, 10 mW, $\lambda = 632.8$ nm) whose light passes through a chopper that is connected to a lock-in amplifier (EG&G 7256). The modulated beam is directed through two polarizers (OWIS) to control the intensity and the plane of polarization of the light. The light is coupled via a high-index prism (Scott, LaSFN9) in the Kretschmann configuration to the backside of the gold-coated substrate, which is optically matched through a refractive-index-matching oil (Cargille; series B; $n_D^{25} = 1.700 \pm 0.0002$) at the prism, mounted on a θ–2θ goniometer in contact with a Teflon cell with a volume of 39 μL and a diameter of 5 mm. The light that leaves the prism passes through a beam splitter; subsequently, the s-polarized light is directed to a reference detector, and the p-polarized light passes through a lens which focuses the light onto a photodiode detector. Laser fluctuations are filtered out by dividing the intensity of the p-polarized light (I_p) by the intensity of the s-polarized light (I_s). All measurements were performed at a constant angle by reflectivity tracking. A Reglo digital MS-4/8 flow pump from Ismatec with four channels was used. In this flow pump, Tygon R3607 tubing with a diameter of 0.76 mm was used, also obtained from Ismatec.

The SPR experiments were performed in a flow cell with a volume of 3.9×10^{-2} mL under flow. Apart from experiments that were flow-rate dependent, a continuous flow of 0.5 mL min^{-1} was used. Before a new experiment was started, the gold substrates were rinsed thoroughly with 10 mM β-CD in 10 mM PBS containing 150 mM NaCl, and 10 mM PBS containing 150 mM NaCl. Experiments were started after the baseline became stable. When the solution had to be changed, the pump was stopped, and switched on again immediately after changing the solution.

μCP: PDMS stamps were prepared by casting a 10:1 (v/v) mixture of poly(dimethylsiloxane) and curing agent (Sylgard 184, Dow Corning) against a patterned silicon master. After curing of the stamps overnight, they were mildly oxidized in an ozone plasma reactor (Ultra-Violet Products Inc., model PR-100) for 60 min to render them hydrophilic. Subsequently, they were inked by soaking them in a 10^{-5} M aqueous solution of the divalent linker (**3**) for 20 min. The master employed to prepare the PDMS stamps had hexagonally oriented 10 μm circular features separated by 5 μm. Before printing, the stamps were blown dry in a stream of N_2. The stamps were applied manually and without pressure control for 10 min onto the β-CD SAMs on gold and then carefully removed. For every printing step, a new stamp was used. The substrates were thoroughly rinsed with water.

AFM: The AFM experiments were performed on a Nanoscope IIIa (Veeco, Digital Instruments, USA) multimode atomic force microscope equipped with a J-scanner (maximum scan size about 170×170 μm^2). The instrument was operated in contact mode setting the feedback mechanism so as to ensure a constant

NANO MICRO small

force between the tip and the sample. The in situ AFM experiments were also performed in tapping mode (non-contact mode) in liquid but the results found were not different from those obtained in contact mode. Commercially available triangular Si_3N_4 cantilevers with a nominal spring constant of about 0.32 $N\,m^{-1}$ were used both in air and in liquid. The total force applied to the surface in air was less than 10 nN. The in situ experiments were performed using a liquid cell supplied by the manufacturer of the instrument. The available volume of the cell was about 50 μL. The sample and the cell were sealed together using a rubber ring. The images were recorded at scan speeds between 1 and 1.5 Hz (1 Hz: 1 line s^{-1}).

Fluorescence microscopy: Fluorescence images were recorded using an Olympus IX71 inverted research microscope equipped with a U-RFL-T mercury burner as light source and an Olympus DP70 digital camera (12.5 million-pixel cooled digital color camera) for image acquisition. Blue excitation light ($450\ nm \leq \lambda \leq 480\ nm$) and green emission light ($\lambda \geq 515\ nm$) was filtered using a U-MWB Olympus filter cube.

XPS spectroscopy: XPS was performed on a PHI Quantera SXM, using a monochromated AlKα X-ray source with an energy of 1486.6 eV. The X-ray beam with a diameter of 100 μm and a power of 25 W was scanned over an area of $300 \times 700\ \mu m^2$. Survey scans (1100–0 eV) were collected at 45° takeoff angle and at a pass energy of 224 eV (0.4 eV step size). Element scans were collected with a pass energy of 112 eV (0.2 eV step size). Samples were neutralized with low-energy Ar^+ ions and electrons. Atomic concentrations were calculated using Multipak 8.0 software from PHI.

Acknowledgements

We are grateful for financial support from the Council for Chemical Sciences of the Netherlands Organization for Scientific Research (NWO-CW) (M.J.W.L; Vidi Vernieuwingsimpuls grant 700.52.423 to J.H.). E. A. Speets is acknowledged for performing the XPS measurements. C. M. Bruinink is acknowledged for supplying the master for the μCP stamps.

[1] K. Zhang, M. R. Diehl, D. A. Tirrell, *J. Am. Chem. Soc.* **2005**, *127*, 10136 – 10137.
[2] H. Zhu, M. Snyder, *Curr. Opin. Chem. Biol.* **2003**, *7*, 55 – 63.
[3] N. L. Rosi, C. A. Mirkin, *Chem. Rev.* **2005**, *105*, 1547 – 1562.
[4] C. M. Niemeyer, *Angew. Chem.* **2001**, *113*, 4254 – 4287; *Angew. Chem. Int. Ed.* **2001**, *40*, 4128 – 4158.
[5] E. Katz, I. Willner, *Angew. Chem.* **2004**, *116*, 6166 – 6235; *Angew. Chem. Int. Ed.* **2004**, *43*, 6042 – 6108.
[6] L. Tiefenauer, R. Ros, *Coll. Surf. B* **2002**, 23, 95 – 114.
[7] W. Knoll, M. Zizlsperger, T. Liebermann, S. Arnold, A. Badia, M. Liley, D. Piscevic, F. J. Schmitt, J. Spinke, *Colloids Surf. A* **2000**, *161*, 115 – 137.
[8] D. Zhou, A. Bruckbauer, L. Ying, C. Abell, D. Klenerman, *Nano Lett.* **2003**, *3*, 1517 – 1520.
[9] A. Chilkoti, P. S. Stayton, *J. Am. Chem. Soc.* **1995**, *117*, 10622 – 10628.
[10] M. González, C. E. Argaraña, G. D. Fidelio, *Biomol. Eng.* **1999**, *16*, 67 – 72.
[11] N. M. Green, *Methods Enzymol.* **1990**, *184*, 51 – 67.
[12] L. A. Klumb, V. Chu, P. S. Stayton, *Biochemistry* **1998**, *37*, 7657 – 7662.
[13] C. Rosano, P. Arosio, M. Bolognesi, *Biomol. Eng.* **1999**, *16*, 5 – 12.
[14] P. C. Weber, M. W. Patoliano, L. D. Thompson, *Biochemistry* **1992**, *31*, 9350 – 9354.
[15] T. Sano, C. R. Cantor, *Proc. Natl. Acad. Sci. USA* **1995**, *92*, 3180 – 3184.
[16] M. J. Swamy, *Biochem. Mol. Biol. Int.* **1995**, *36*, 219 – 225.
[17] M. González, L. A. Bagatolli, I. Echabe, J. L. R. Arrondo, C. E. Argaraña, C. R. Cantor, G. D. Fidelio, *J. Biol. Chem.* **1997**, *272*, 11288 – 11294.
[18] W. A. Hendrickson, A. Pähler, J. L. Smith, Y. Satow, E. A. Merritt, *Proc. Natl. Acad. Sci. USA* **1989**, *86*, 2190 – 2194.
[19] A. Biebricher, A. Paul, P. Tinnefeld, A. Gölzhäuser, M. Sauer, *J. Biotechnol.* **2004**, *112*, 97 – 107.
[20] I. T. Dorn, K. R. Neumaier, R. Tampé, *J. Am. Chem. Soc.* **1998**, *120*, 2753 – 2763.
[21] J. F. Hainfeld, W. Liu, *J. Struct. Biol.* **1999**, *127*, 185 – 198.
[22] U. Rädler, J. Mack, N. Persike, G. Jung, R. Tampé, *Biophys. J.* **2000**, *79*, 3144 – 3152.
[23] L. Schmitt, C. Dietrich, R. Tampé, *J. Am. Chem. Soc.* **1994**, *116*, 8485 – 8491.
[24] S. Lata, A. Reichert, R. Brock, R. Tampé, J. Piehler, *J. Am. Chem. Soc.* **2005**, *127*, 10205 – 10215.
[25] A. Tinazli, J. Tang, R. Valiokas, S. Pićurić, S. Lata, J. Piehler, B. Liedberg, R. Tampé, *Chem. Eur. J.* **2005**, *11*, 5249 – 5259.
[26] R. Blankenburg, P. Meller, H. Ringsdorf, C. Salesse, *Biochemistry* **1989**, *28*, 8214 – 8221.
[27] S. A. Darst, M. Ahlers, P. H. Meller, E. W. Kubalek, R. Blankenburg, H. O. Ribi, H. Ringsdorf, R. D. Kornberg, *Biophys. J.* **1991**, *59*, 387 – 396.
[28] P. L. Edmiston, S. S. Saavedra, *J. Am. Chem. Soc.* **1998**, *120*, 1665 – 1671.
[29] A. Schmidt, J. Spinke, E. Bayerl, W. Knoll, *Biophys. J.* **1992**, *63*, 1185 – 1192.
[30] S. Zhao, W. M. Reichert, *Langmuir* **1992**, *8*, 2785 – 2791.
[31] W. Müller, H. Ringsdorf, E. Rump, X. Zhang, L. Angermaier, W. Knoll, J. Spinke, *J. Biomater. Sci. Polym. Ed.* **1994**, *6*, 481 – 495.
[32] M. V. Rekharsky, Y. Inoue, *Chem. Rev.* **1998**, *98*, 1880 – 1901.
[33] M. W. J. Beulen, J. Bügler, B. Lammerink, F. A. J. Geurts, E. M. E. F. Biemond, K. G. C. van Leerdam, F. C. J. M. van Veggel, J. F. J. Engbersen, D. N. Reinhoudt, *Langmuir* **1998**, *14*, 6424 – 6429.
[34] M. W. J. Beulen, J. Bügler, M. R. de Jong, B. Lammerink, J. Huskens, H. Schönherr, G. J. Vancso, B. A. Boukamp, H. Wieder, A. Offenhäuser, W. Knoll, F. C. J. M. van Veggel, D. N. Reinhoudt, *Chem. Eur. J.* **2000**, *6*, 1176 – 1183.
[35] J. Huskens, A. Mulder, T. Auletta, C. A. Nijhuis, M. J. W. Ludden, D. N. Reinhoudt, *J. Am. Chem. Soc.* **2004**, *126*, 6784 – 6797.
[36] T. Auletta, B. Dordi, A. Mulder, A. Sartori, S. Onclin, C. M. Bruinink, M. Péter, C. A. Nijhuis, H. Beijleveld, H. Schönherr, G. J. Vancso, A. Casnati, R. Ungaro, B. J. Ravoo, J. Huskens, D. N. Reinhoudt, *Angew. Chem.* **2004**, *116*, 373 – 376; *Angew. Chem. Int. Ed.* **2004**, *43*, 369 – 373.
[37] J. Huskens, M. A. Deij, D. N. Reinhoudt, *Angew. Chem.* **2002**, *114*, 4647 – 4651; *Angew. Chem. Int. Ed.* **2002**, *41*, 4467 – 4471.
[38] C. A. Nijhuis, F. Yu, W. Knoll, J. Huskens, D. N. Reinhoudt, *Langmuir* **2005**, *21*, 7866 – 7876.
[39] A. Mulder, S. Onclin, M. Péter, J. P. Hoogenboom, H. Beijleveld, J. ter Maat, M. F. García-Parajó, B. J. Ravoo, J. Huskens, N. F. van Hulst, D. N. Reinhoudt, *Small* **2005**, *1*, 242 – 253.
[40] F. Corbellini, A. Mulder, A. Sartori, M. J. W. Ludden, A. Casnati, R. Ungaro, J. Huskens, M. Crego-Calama, D. N. Reinhoudt, *J. Am. Chem. Soc.* **2004**, *126*, 17050 – 17058.

[41] S. Onclin, A. Mulder, J. Huskens, B. J. Ravoo, D. N. Reinhoudt, *Langmuir* **2004**, *20*, 5460 – 5466.
[42] A. Cooper, *J. Am. Chem. Soc.* **1992**, *114*, 9208 – 9209.
[43] A. Cooper, M. Lovatt, M. A. Nutley, *J. Inclusion Phenom.* **1985**, *3*, 189 – 192.
[44] D. Rozema, S. H. Gellman, *J. Am. Chem. Soc.* **1995**, *117*, 2373 – 2374.

Received: March 28, 2006
Revised: May 12, 2006
Published online on August 17, 2006

